

https://doi.org/10.1130/G49451.1

Manuscript received 1 July 2021 Revised manuscript received 1 November 2021 Manuscript accepted 19 November 2021

Published online 25 February 2022

© 2022 The Authors. Gold Open Access: This paper is published under the terms of the CC-BY license.

History of earthquakes along the creeping section of the San Andreas fault, California, USA

Genevieve L. Coffey^{1*}, Heather M. Savage², Pratigya J. Polissar³, Stephen E. Cox⁴, Sidney R. Hemming⁴, Gisela Winckler⁴ and Kelly K. Bradbury⁵

¹GNS Science, 1 Fairway Drive, Lower Hutt 5011, New Zealand

ABSTRACT

Creeping faults are difficult to assess for seismic hazard because they may participate in rupture even though they likely cannot nucleate large earthquakes. The creeping central section of the San Andreas fault in California (USA) has not participated in a historical large earthquake; however, earthquake ruptures nucleating in the locked northern and southern sections may propagate through the creeping section. We used biomarker thermal maturity and K/Ar dating on samples from the San Andreas Fault Observatory at Depth to look for evidence of earthquakes. Biomarkers show evidence of many earthquakes with displacements >1.5 m in and near a 3.5-m-wide patch of the fault. We show that K/Ar ages decrease with thermal maturity, and partial resetting occurs during coseismic heating. Therefore, measured ages provide a maximum constraint on earthquake age, and the youngest earthquakes here are younger than 3 Ma. Our results demonstrate that creeping faults may host large earthquakes over longer time scales.

INTRODUCTION

The San Andreas fault (SAF) in California (USA) exhibits stark contrasts in slip style along its length (Fig. 1A). The northern and southern sections are locked and have hosted large earthquakes, including the $M_{\rm w}$ 7.9 1906 San Francisco earthquake. The central SAF, on the other hand, releases elastic strain through aseismic creep (Titus et al., 2006). Large earthquakes are not thought to nucleate along this segment; however, if a large earthquake initiates on either the northern or southern section and propagates into the central creeping section, it is possible that the central SAF may become unstable and fail coseismically (Noda and Lapusta, 2013). Propagation through the central SAF would allow for the possibility of a whole-fault rupture, increasing the maximum-magnitude earthquake possible on the SAF to $> M_{w}$ 8 and raising the overall seismic hazard of California (Cui et al.,

*E-mail: g.coffey@gns.cri.nz

We can investigate the longer-term seismic history of the central SAF by turning to evidence of past earthquakes in the rock record. Due to the frictional resistance of faults, heat is rapidly generated during coseismic slip, leading to temperature spikes (Rowe and Griffith, 2015). Utilizing this relationship, we identified evidence of frictional heating during earthquakes through the creeping section of the SAF in cores col-

lected at the San Andreas Fault Observatory at Depth (SAFOD, https://earthquake.usgs.gov/learn/parkfield/safod_pbo.php; Figs. 1B–1D). Using biomarker thermal maturity and K/Ar ages of illite from the SAFOD cores, we show that a patch of the fault has experienced abundant seismicity over the past ~16 m.y.

Coseismic Temperature Rise and the Chemistry of Faults

Faults heat up coseismically as a function of the earthquake source parameters—shear stress, displacement, and slip velocity—as well as fault properties, including thickness of the slipping zone and material properties of the rocks. Biomarkers have historically been used in petroleum studies to assess the maturity of hydrocarbon-bearing source rocks, which undergo heating due to burial. However, they can also be used to analyze the maturity of rocks that have been heated at higher temperatures over shorter earthquake durations (Savage et al., 2014, 2018; Rabinowitz et al., 2017).

We analyzed a suite of biomarker maturity indices in the rocks from SAFOD and focused on methylphenanthrenes (MPs; Fig. 2; Figs. S1–S7 in the Supplemental Material¹). Because biomarkers experience structural changes during heating, we can quantify thermal maturity using the increase in abundance of the thermally stable isomers of these biomarkers with increasing temperature (Szczerba and Rospondek, 2010; Polissar et al., 2011):

$$MPI4 = \frac{3MP + 2MP}{3MP + 2MP + 9MP + 1MP},$$
 (1)

containing model parameters and biomarker data. Please visit https://doi.org/10.1130/GEOL.S.18174665 to access the supplemental material, and contact editing@geosociety.org with any questions.

CITATION: Coffey, G.L., et al., 2022, History of earthquakes along the creeping section of the San Andreas fault, California, USA: Geology, v. 50, p. 516-521, https://doi.org/10.1130/G49451.1

²Department of Earth & Planetary Science, University of California-Santa Cruz, 1156 High Street, Santa Cruz, California 95064, USA

³Department of Ocean Sciences, University of California-Santa Cruz, 1156 High Street, Santa Cruz, California 95063, USA

⁴Lamont-Doherty Earth Observatory of Columbia University, 61 Route 9W, Palisades, New York 10964, USA

Department of Geosciences, Utah State University, 4505 Old Main Hill, Logan, Utah 84322, USA

^{2010).} Historically, this part of the fault has not hosted a large earthquake ($M_w > 6$), and paleoseismic trenching in this region has revealed no evidence of surface-rupturing earthquakes in the past 2000 yr (Toké et al., 2006). However, this is a short seismic record, and studies have demonstrated the potential for coseismic slip over longer periods (Harris, 2017). Interferometric synthetic aperture radar (INSAR) and GPS measurements reveal creep deficits in the crust ($\sim 10-20~\rm km$ depth), indicating that locked patches are present and accumulating strain (Maurer and Johnson, 2014).

Supplemental Material. Supplemental figures related to biomarker analysis, thermal modeling, and experimental setup; more detailed methodology, and tables

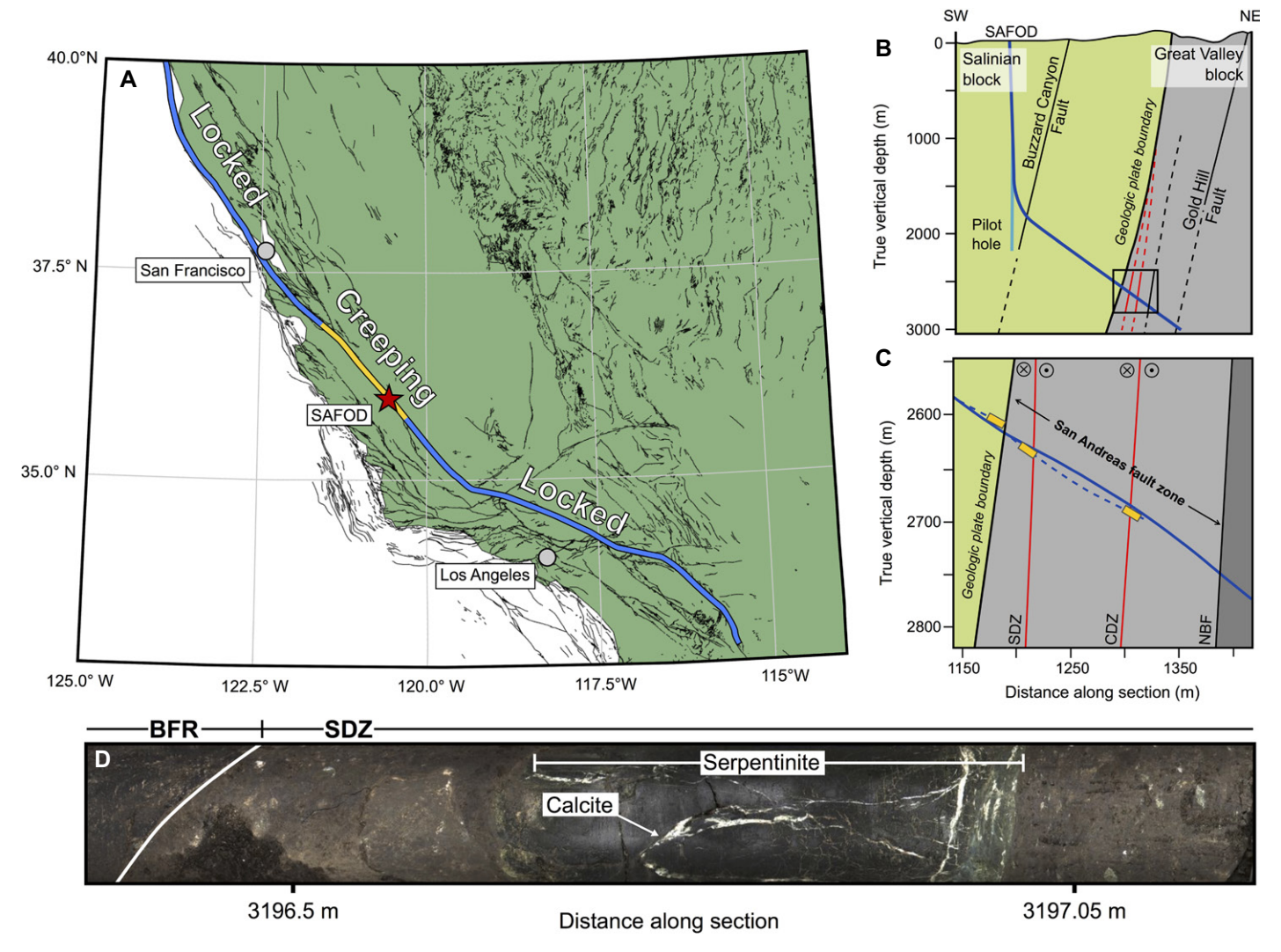


Figure 1. (A) Map of the San Andreas fault (SAF) showing locked (blue) and creeping (yellow) sections. Black lines are other active faults (from U.S. Geological Survey and California Geological Survey, https://www.usgs.gov/natural-hazards/earthquake-hazards/faults/, accessed November 2019). (B,C) Cross sections of drilling at the San Andreas Fault Observatory at Depth (SAFOD, https://earthquake.usgs.gov/learn/parkfield/safod_pbo.php) modified from Hickman et al. (2007). Fault zone is indicated in gray and includes everything to the right of the contact between the Salinian block (green) and Great Valley Sequence (GVS) to the northern boundary fault (NBF). The southern deforming zone (SDZ) and central deforming zone (CDZ) are indicated. Blue line is the path of SAFOD drilling, and yellow boxes are where cores were collected. (D) Photograph of a core from the SAFOD containing black fault rock (BFR) and the western side of actively creeping SDZ.

where 2MP and 3MP are the thermally stable isomers, and 9MP and 1MP are the thermally unstable isomers. The kinetics of MP reaction with temperature rise allow MPI4 to be linked to the time and temperature conditions of an earthquake (Sheppard et al., 2015). When interpreting MPI4, we assumed any heating signal was a result of the largest event the fault has experienced, because any smaller events will have lower effect on the overall maturity due to the strong temperature dependence of the kinetics (Coffey et al., 2019).

While biomarkers can be used to identify past earthquakes in the rock record, they do not provide information on earthquake timing. Recent advances in our understanding of geochronology in fault studies have led to the development of a number of different dating tools, including ⁴⁰Ar/³⁹Ar dating of illite gouge

(van der Pluijm et al., 2001; Schleicher et al., 2010) and (U-Th)/He dating of hematite fault surfaces (Ault et al., 2015). Although ⁴⁰Ar/³⁹Ar is the analytically preferable method for argon geochronology, we used the K/Ar method here due to argon recoil effects associated with clay grain sizes (van der Pluijm et al., 2001). Like biomarker indices, we show experimentally that thermal resetting of K/Ar ages in illite requires much higher temperatures over the short durations of earthquakes than over geologic time scales.

RESULTS Earthquake Evidence at SAFOD

MPs within the SAFOD core show a clear background maturity (0.41–0.51; Fig. 2A) due to burial heating. Between 3192 and 3196 m, MPI4 values are much higher than background,

ranging from 0.54 to 0.67 (Fig. 2A), with lower values toward the edges. Such a localized maturity signal requires a high-temperature, shortduration heating event like an earthquake. Other transient heat sources such as hydrothermal fluids are unlikely to cause this signal because paleofluid temperatures measured from calcite veins are consistent with background temperatures (Luetkemeyer et al., 2016), and there is no mineralogic evidence such as authigenic muscovite or epidote. The high-thermal-maturity region is asymmetric, with higher thermal maturities closer to the southern deforming zone (SDZ), and it occurs mostly within a region of pervasive deformation, previously described as a black fault rock (BFR; Bradbury et al., 2011). The BFR consists of a black ultracataclasite with scaly fabric, and it contains many polished, highly reflective slip layers (Bradbury

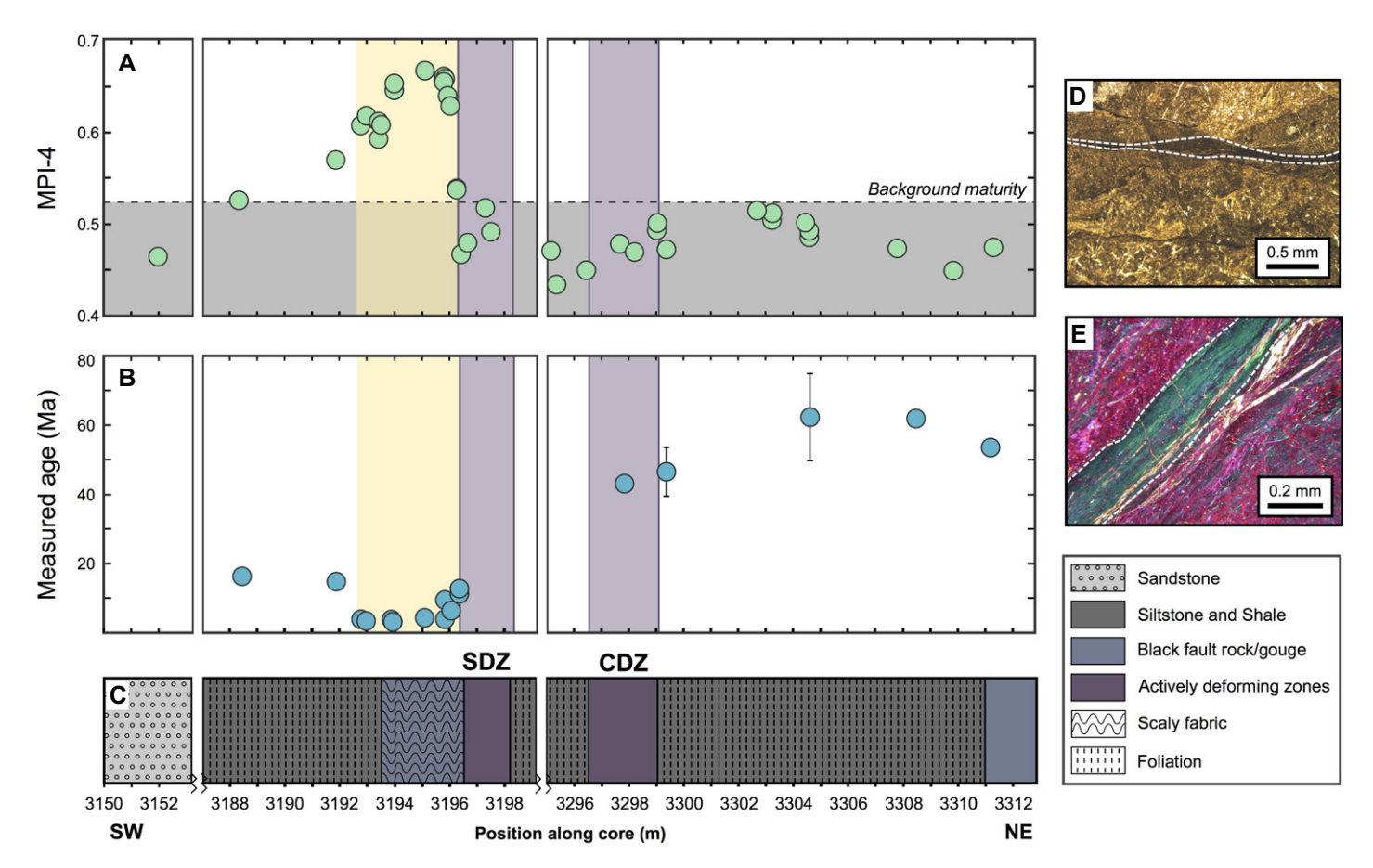


Figure 2. (A) Methylphenanthrene index (MPI4) along analyzed sections of the San Andreas Fault Observatory at Depth (SAFOD) core (analytical uncertainties are less than symbol size). Purple shaded regions are the southern deforming zone (SDZ) and central deforming zone (CDZ); yellow shaded area is a region of high thermal maturity. (B) Measured K/Ar ages (error bars represent 2σ standard deviation; where these are not shown, they are smaller than symbol size). (C) Schematic SAFOD lithology, modified from Bradbury et al. (2011). Breaks in the x axis are gaps between cored sections. (D,E) Photomicrographs of slip layers in black fault rock (BFR) at 3194.8 and 3196 m depth, respectively. Photo in D was taken using plane light, and a gypsum plate was inserted for E. Slip layers in D and E are outlined by white dashed lines.

et al., 2011; Fig. 1D), suggesting the occurrence of abundant slip within this interval. Using transmitted light and scanning electron microscopy, we determined that slip layer thickness varies from $100~\mu m$ to 1.8~cm (average = 2~mm). Previous studies show that high temperatures are typically restricted to micrometer- and millimeter-thick layers during earthquakes (Savage et al., 2018; Coffey et al., 2019; Savage and Polissar, 2019). Therefore, given the abundance of slip layers and spread of high maturities across the BFR, it is very likely that this zone has hosted many (>100) earthquakes

How Large Were the Earthquakes In and Near the Black Fault Rock?

We estimated temperatures within the BFR by modeling heat generation and diffusion along a slip layer (Lachenbruch, 1986; Fulton and Harris, 2012; see the Supplemental Material). Coupling this modeling with MP reaction kinetics allowed us to forward model biomarker reaction for different earthquake properties and identify the thermal maturity and temperature profiles that best fit our measurements (Sheppard et al., 2015). No evidence of bulk melting has been

documented in the SAFOD cores; therefore, we capped temperatures at 1100 °C (Srinivasachar et al., 1990). The mean maximum temperature modeled for the reacted samples was 840 °C (95% confidence interval [CI] of 570–1100 °C; Fig. 3A; Fig. S9). Using best-fitting temperature profiles along with thermal and fault parameters (Table S1), we placed constraints on earthquake displacement through this patch assuming an average friction of 0.1-0.2 (Fig. S12). Our models showed that possible displacements for each sample fall into a 95% confidence interval of 0.5-2.9 m (Fig. 3B). Uncertainties in friction, thickness of the slipping layer (Figs. 2D and 2E), and the reaction kinetics of MPI4 led to the wide range of possible displacements that matched our signal. The lower end of these displacements is consistent with M_w 6 Parkfieldsized earthquakes, and this may mean that some Parkfield events have propagated this far into the creeping section. However, given that we expect the average friction during most modeled events to be close to 0.1 (Fig. S12), most earthquakes in this patch would have an average displacement of 1.5 m, which corresponds to earthquakes of $> M_w 6.9$ (see the Supplemental

Material). Therefore, it is likely that many of these earthquakes were larger-magnitude events than the Parkfield events.

Despite sampling along 41 m of the SAF, we found evidence of seismicity only within and adjacent to the \sim 3.5-m-wide BFR. It is unclear why earthquakes continually rupture through this patch instead of the frictionally weaker SDZ or CDZ (central deforming zone; Carpenter et al., 2011). While it is possible earthquakes occurred in unsampled regions of the fault zone, the BFR appears to be susceptible to earthquake rupture that does not occur elsewhere in the sampled intervals. Proximity to a bimaterial interface between Salinian and Great Valley Sequence (GVS) rocks may lead to earthquake localization close to this boundary, as suggested by Ben-Zion (2008) and documented previously in other fault zones (Rabinowitz et al., 2020).

When Did Earthquakes Occur In and Near the Black Fault Rock?

The measured K/Ar ages within bulk samples from the SAFOD core range from 62.3 Ma to 3.2 Ma (Fig. 2B). These ages can be split

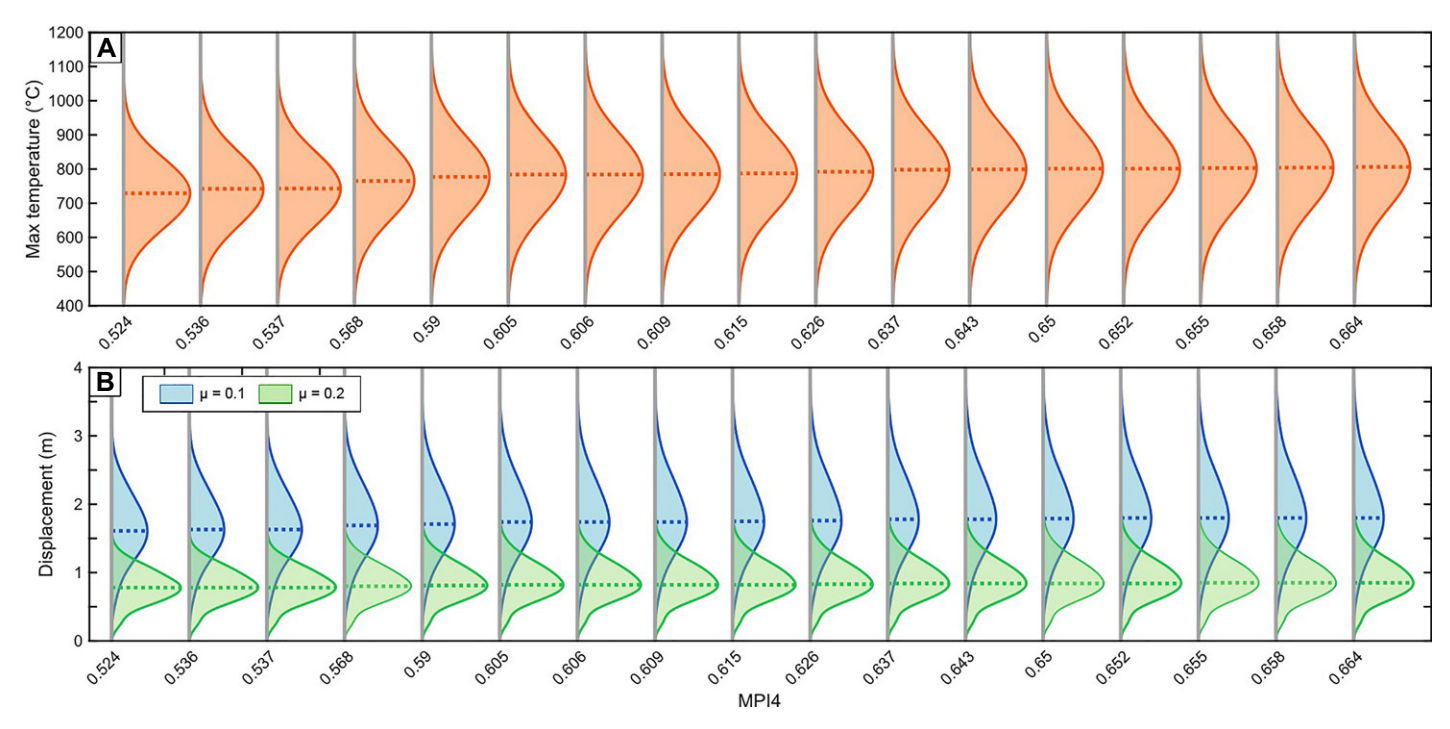


Figure 3. (A) Probability distribution functions (PDFs) of maximum temperature modeled for each reacted sample. PDF width is largely due to uncertainties in methylphenanthrene index (MPI4) kinetics (see the Supplemental Material [see footnote 1]). (B) Possible earthquake displacements for $\mu = 0.1$ (blue) and $\mu = 0.2$ (green) cases. Dotted lines in each plot are the most likely temperatures and displacements.

into three distinct populations: those that lie within the BFR, those in the deforming zones, and those in the background GVS. The mean age of the GVS is 56.1 Ma, with ages ranging between 62.3 and 46.5 Ma. The oldest of our ages are consistent with reported ages of the GVS (Dickinson and Rich, 1972). Ages within the CDZ are slightly younger, with a mean age of 38.4 Ma (43.1–33.8 Ma). A sample from the SDZ was also measured, but it contained a large amount of air and very little potassium, so it is not included here. Ages in the CDZ are

consistent with GVS ages but are younger than background samples, possibly due to authigenic illite produced by continuous deformation and fluid-rock interaction during aseismic creep (Schleicher et al., 2010). The youngest K/Ar ages occur within and adjacent to the BFR (9.5–3.3 Ma) and are slightly older in the two thermally mature samples northeast of the BFR (16–15 Ma). We observed that the youngest ages occurred in samples with the highest MPI4 (Fig. 4A), indicating that the high temperatures identified from biomarkers also led to partial or

complete resetting of the K/Ar chronometer. As a result, we infer that these samples have experienced at least some resetting during coseismic slip and reflect maximum earthquake ages.

In order to further investigate whether the measured ages within the heated region reflect the timing of earthquake slip, we performed a series of rapid heating experiments to explore the relationship between argon degassing and temperature. Experiments were performed on a 62.3 Ma GVS sample with a background MPI4, which was not affected by earthquake heating.

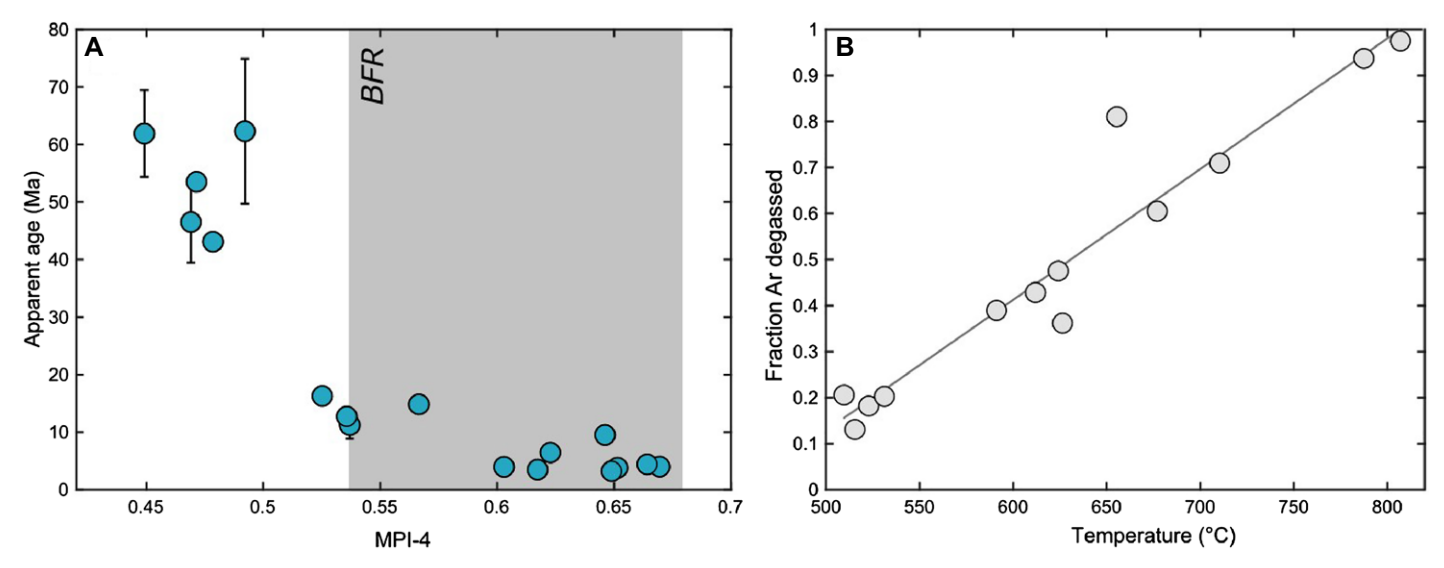


Figure 4. (A) Measured ages plotted against the methylphenanthrene index (MPI4) showing a clear negative relationship between age and MPI4, and hence age and temperature rise. Gray region encompasses samples collected from black fault rock (BFR). (B) Fraction of argon released as a function of temperature from the heating experiments.

We used a diode laser to heat the sample to temperatures of 500-820 °C for 10 s to directly simulate earthquake conditions and measured the fraction of argon released (Fig. 4B; see the Supplemental Material). The results of these experiments support the inference that K/Ar ages are reset during short-duration heating events and that the fraction of argon released is a simple function of temperature when time is held constant. Argon loss during heating occurred at temperatures above 500 °C, and complete degassing occurred by ~ 800 °C (Fig. 4B). While these temperatures are like those modeled for SAFOD (Fig. 3A), we do not have constraints on the slip duration, and hence heating duration, at SAFOD. However, with modeled displacements of up to 2.9 m and a slip velocity of \sim 1 m s⁻¹ (Heaton, 1990), the heating duration of our experiments was likely longer than the duration of coseismic heating at SAFOD. Therefore, these results likely reflect partial resetting of K/Ar ages at SAFOD, as shown by Figure 4A, and measured ages can be treated as maximum earthquake ages, but true earthquake ages are likely younger.

DISCUSSION

We have shown that there is ample evidence for earthquake slip within and around the BFR since 16 Ma. Although there is no consensus on how long the creeping section has persisted, analysis of deformed Quaternary sediments suggests that the central SAF has been creeping for at least 2 m.y. (Titus et al., 2011) and possibly up to 5 m.y. (d'Alessio et al., 2006). Therefore, some of the earthquakes identified here may have occurred when the central SAF was locked. However, several of the measured K/Ar ages are younger than 5 Ma, and if partially reset, other measured ages fall within this interval and reflect propagation of large-displacement earthquakes into the creeping section. An alternative explanation could be that the creep only began ca. 3 Ma, which is the youngest measured age of the inferred earthquakes. However, as stated above, these earthquakes ages could be much younger.

It is also possible that some of the older inferred earthquakes originally occurred along the locked southern SAF before the BFR block was translated to its present-day position at SAFOD. The central SAF at its southern end creeps at a rate of ~26 mm/yr (Toké et al., 2011), meaning it would take 1.5 m.y. to transport the BFR 40 km from the locked portion of the fault at Cholame to the SAFOD site. However, we think it is unlikely that the fault rock would move in one direction over geologic time. The BFR is located within the fault zone, and as localized slip zones migrate around over time, it could be translated with the Pacific plate or the North American plate. Despite being on the Pacific plate side of the actively deforming SDZ and CDZ, displacement that occurred between the BFR and the Salinian block (of which there is ample evidence in the SAFOD core) would move the BFR relatively southeast.

A fundamental takeaway from this work is that by combining independent temperature proxies with thermochronology and detailed textural observations, we can access the seismic history of the SAF over millions of years. This provides a powerful new method for conducting paleoseismology on the >100,000 yr time scale. In doing this, we show that large (displacement >1.5 m) earthquakes have repeatedly ruptured the rocks at SAFOD, and K/Ar dating of fault rocks can constrain these earthquakes to within the past 16-3 m.y. Furthermore, biomarkers demonstrate that earthquakes were localized outside of the weak deforming zones, suggesting that fault zones can fail in different slip styles across their width, and major earthquakes may occur along creeping faults, provided that some strain accumulates. Ultimately, our work points to the potential for higher-magnitude earthquakes in central California and highlights the importance of including the central SAF and other creeping faults in seismic hazard analysis.

ACKNOWLEDGMENTS

We are grateful to Nicole deRoberts, Tanzhou Liu, Roseanne Schwartz, and Chiza Mwinde for laboratory assistance. This study was supported by the U.S. National Science Foundation Earthscope program (grant EAR1358585), the Southern California Earthquake Center (grant SCEC no. 14112), the Brinson Foundation (Chicago, Illinois), and the "Elsevier Research Scholarship, sponsored by the journal *Organic Geochemistry* and Elsevier.

REFERENCES CITED

- Ault, A.K., Reiners, P.W., Evans, J.P., and Thomson, S.N., 2015, Linking hematite (U-Th)/ He dating with the microtextural record of seismicity in the Wasatch fault damage zone, Utah, USA: Geology, v. 43, p. 771–774, https://doi.org/10.1130/ G36897.1.
- Ben-Zion, Y., 2008, Collective behavior of earthquakes and faults: Continuum-discrete transitions, progressive evolutionary changes, and different dynamic regimes: Reviews of Geophysics, v. 46, RG4006, https://doi.org/10.1029 /2008RG000260.
- Bradbury, K.K., Evans, J.P., Chester, J.S., Chester, F.M., and Kirschner, D.L., 2011, Lithology and internal structure of the San Andreas fault at depth based on characterization of Phase 3 whole-rock core in the San Andreas Fault Observatory at Depth (SAFOD) borehole: Earth and Planetary Science Letters, v. 310, p. 131–144, https://doi.org/10.1016/j.epsl.2011.07.020.
- Carpenter, B.M., Marone, C., and Saffer, D.M., 2011, Weakness of the San Andreas fault revealed by samples from the active fault zone: Nature Geoscience, v. 4, p. 251–254, https://doi.org/10.1038 /ngeo1089.
- Coffey, G.L., Savage, H.M., Polissar, P.J., Rowe, C.D., and Rabinowitz, H.S., 2019, Hot on the trail: Coseismic heating on a localized structure along the Muddy Mountain fault, Nevada: Journal of Structural Geology, v. 120, p. 67–79, https://doi.org/10.1016/j.jsg.2018.12.012.
- Cui, Y., et al., 2010, Scalable earthquake simulation on petascale supercomputers, *in* SC '10: Proceedings

- of the 2010 ACM/IEEE International Conference for High Performance Computing, Networking, Storage and Analysis, November 2010: IEEE, p. 1–20, https://doi.org/10.1109/SC.2010.45.
- d'Alessio, M.A., Williams, C.F., and Bürgmann, R., 2006, Frictional strength heterogeneity and surface heat flow: Implications for the strength of the creeping San Andreas fault: Journal of Geophysical Research: Solid Earth, v. 111, B05410, https://doi.org/10.1029/2005JB003780.
- Dickinson, W.R., and Rich, E.I., 1972, Petrologic intervals and petrofacies in the Great Valley Sequence, Sacramento Valley, California: Geological Society of America Bulletin, v. 83, p. 3007–3024, https://doi.org/10.1130/0016-7606(1972)83[3007:PIAPIT]2.0.CO;2.
- Fulton, P.M., and Harris, R.N., 2012, Thermal considerations in inferring frictional heating from vitrinite reflectance and implications for shallow coseismic slip within the Nankai subduction zone: Earth and Planetary Science Letters, v. 335, p. 206–215, https://doi.org/10.1016/j.epsl.2012.04.012.
- Harris, R.A., 2017, Large earthquakes and creeping faults: Reviews of Geophysics, v. 55, p. 169–198, https://doi.org/10.1002/2016RG000539.
- Hickman, S., Zoback, M.D., Ellsworth, W., Boness, N., Malin, P., Roecker, S., and Thurber, C., 2007, Structure and properties of the San Andreas fault in central California: Recent results from the SAFOD experiment: Scientific Drilling, Special Issue, p. 29–32, https://doi.org/10.5194/sd-SpecialIssue-29-2007.
- Lachenbruch, A.H., 1986, Simple Models for the Estimation and Measurement of Frictional Heating by an Earthquake: U.S. Geological Survey Open-File Report 86-508, 13 p., https://doi.org/10.3133/ofr86508.
- Luetkemeyer, P.B., Kirschner, D.L., Huntington, K.W., Chester, J.S., Chester, F.M., and Evans, J.P., 2016, Constraints on paleofluid sources using the clumped-isotope thermometry of carbonate veins from the SAFOD (San Andreas Fault Observatory at Depth) borehole: Tectonophysics, v. 690, p. 174–189, https://doi.org/10.1016/j.tecto .2016.05.024.
- Maurer, J., and Johnson, K., 2014, Fault coupling and potential for earthquakes on the creeping section of the central San Andreas fault: Journal of Geophysical Research: Solid Earth, v. 119, p. 4414–4428, https://doi.org/10.1002/2013JB010741.
- Noda, H., and Lapusta, N., 2013, Stable creeping fault segments can become destructive as a result of dynamic weakening: Nature, v. 493, p. 518–521, https://doi.org/10.1038/nature11703.
- Polissar, P.J., Savage, H.M., and Brodsky, E.E., 2011, Extractable organic material in fault zones as a tool to investigate frictional stress: Earth and Planetary Science Letters, v. 311, p. 439–447, https://doi.org/10.1016/j.epsl.2011.09.004.
- Rabinowitz, H.S., Polissar, P., and Savage, H., 2017, Reaction kinetics of alkenone and *n*-alkane thermal alteration at seismic timescales: Geochemistry Geophysics Geosystems, v. 18, p. 204–219, https://doi.org/10.1002/2016GC006553.
- Rabinowitz, H.S., Kirkpatrick, J.D., Savage, H.M., Polissar, P.J., and Rowe, C.D., 2020, Earthquake slip surfaces identified by biomarker thermal maturity within the 2011 Tohoku-Oki earthquake fault zone: Nature Communications, v. 11, p. 1–9, https://doi.org/10.1038/s41467-020-14447-1.
- Rowe, C.D., and Griffith, W.A., 2015, Do faults preserve a record of seismic slip: A second opinion: Journal of Structural Geology, v. 78, p. 1–26, https://doi.org/10.1016/j.jsg.2015.06.006.
- Savage, H.M., and Polissar, P.J., 2019, Biomarker thermal maturity reveals localized temperature

- rise from paleoseismic slip along the Punchbowl fault, CA, USA: Geochemistry Geophysics Geosystems, v. 20, p. 3201–3215, https://doi.org/10.1029/2019GC008225.
- Savage, H.M., Polissar, P.J., Sheppard, R., Rowe, C.D., and Brodsky, E.E., 2014, Biomarkers heat up during earthquakes: New evidence of seismic slip in the rock record: Geology, v. 42, p. 99–102, https://doi.org/10.1130/G34901.1.
- Savage, H.M., Rabinowitz, H.S., Spagnuolo, E., Aretusini, S., Polissar, P.J., and Di Toro, G., 2018, Biomarker thermal maturity experiments at earthquake slip rates: Earth and Planetary Science Letters, v. 502, p. 253–261, https://doi.org/10.1016/j.epsl.2018.08.038.
- Schleicher, A.M., van Der Pluijm, B.A., and Warr, L.N., 2010, Nanocoatings of clay and creep of the San Andreas fault at Parkfield: California Geology, v. 38, p. 667–670, https://doi.org/10.1130/G31091.1.
- Sheppard, R.E., Polissar, P.J., and Savage, H.M., 2015, Organic thermal maturity as a proxy for frictional fault heating: Experimental constraints on methylphenanthrene kinetics at earthquake

- timescales: Geochimica et Cosmochimica Acta, v. 151, p. 103–116, https://doi.org/10.1016/j.gca.2014.11.020.
- Srinivasachar, S., Helble, J.J., Boni, A.A., Shah, N., Huffman, G.P., and Huggins, F.E., 1990, Mineral behavior during coal combustion: 2. Illite transformations: Progress in Energy and Combustion Science, v. 16, p. 293–302, https://doi.org/10.1016/0360-1285(90)90038-5.
- Szczerba, M., and Rospondek, M.J., 2010, Controls on distributions of methylphenanthrenes in sedimentary rock extracts: Critical evaluation of existing geochemical data from molecular modelling: Organic Geochemistry, v. 41, p. 1297–1311, https://doi.org/10.1016/j.orggeochem.2010.09.009.
- Titus, S.J., Demets, C., and Tikoff, B., 2006, Thirty-five-year creep rates for the creeping segment of the San Andreas fault and the effects of the 2004 Parkfield earthquake: Constraints from alignment arrays, continuous global positioning system, and creepmeters: Bulletin of the Seismological Society of America, v. 96, p. 250–268, https://doi.org/10.1785/0120050811.

- Titus, S.J., Dyson, M., DeMets, C., Tikoff, B., Rolandone, F., and Bürgmann, R., 2011, Geologic versus geodetic deformation adjacent to the San Andreas fault, central California: Geological Society of America Bulletin, v. 123, p. 794–820, https://doi.org/10.1130/B30150.1.
- Toké, N.A., Arrowsmith, J.R., Rymer, M.J., Landgraf, A., Haddad, D.E., Busch, M., et al., 2011, Late Holocene slip rate of the San Andreas fault and its accommodation by creep and moderate-magnitude earthquakes at Parkfield, California: Geology, v. 39, p. 243–246, https://doi.org/10.1130/G31498.1.
- Toké, N.A., Arrowsmith, J.R., Young, J.J., and Crosby, C.J., 2006, Paleoseismic and postseismic observations of surface slip along the Parkfield segment of the San Andreas fault: Bulletin of the Seismological Society of America, v. 96, 4B, p. S221– S238, https://doi.org/10.1785/0120050809.
- van der Pluijm, B.A., Hall, C.M., Vrolijk, P.J., Pevear, D.R., and Covey, M.C., 2001, The dating of shallow faults in the Earth's crust: Nature, v. 412, p. 172–175, https://doi.org/10.1038/35084053.

Printed in USA